Supplementary Information Appendix for

Depletion interactions modulate the binding between disordered proteins in crowded environments

Franziska Zosel[1,2], Andrea Soranno[1,3], Karin J. Buholzer[1], Daniel Nettels[1], & Benjamin Schuler[1,4]

[1]Department of Biochemistry, University of Zurich, Winterthurerstrasse 190, 8057 Zurich, Switzerland
[2]Current Address: Novo Nordisk A/S, Novo Nordisk Park, 2760 Måløv, Denmark
[3]Department of Biochemistry and Molecular Biophysics, Washington University in St. Louis, Missouri 63130, United States
[4]Department of Physics, University of Zurich, Winterthurerstrasse 190, 8057 Zurich, Switzerland

www.pnas.org/cgi/doi/10.1073/pnas.1921617117

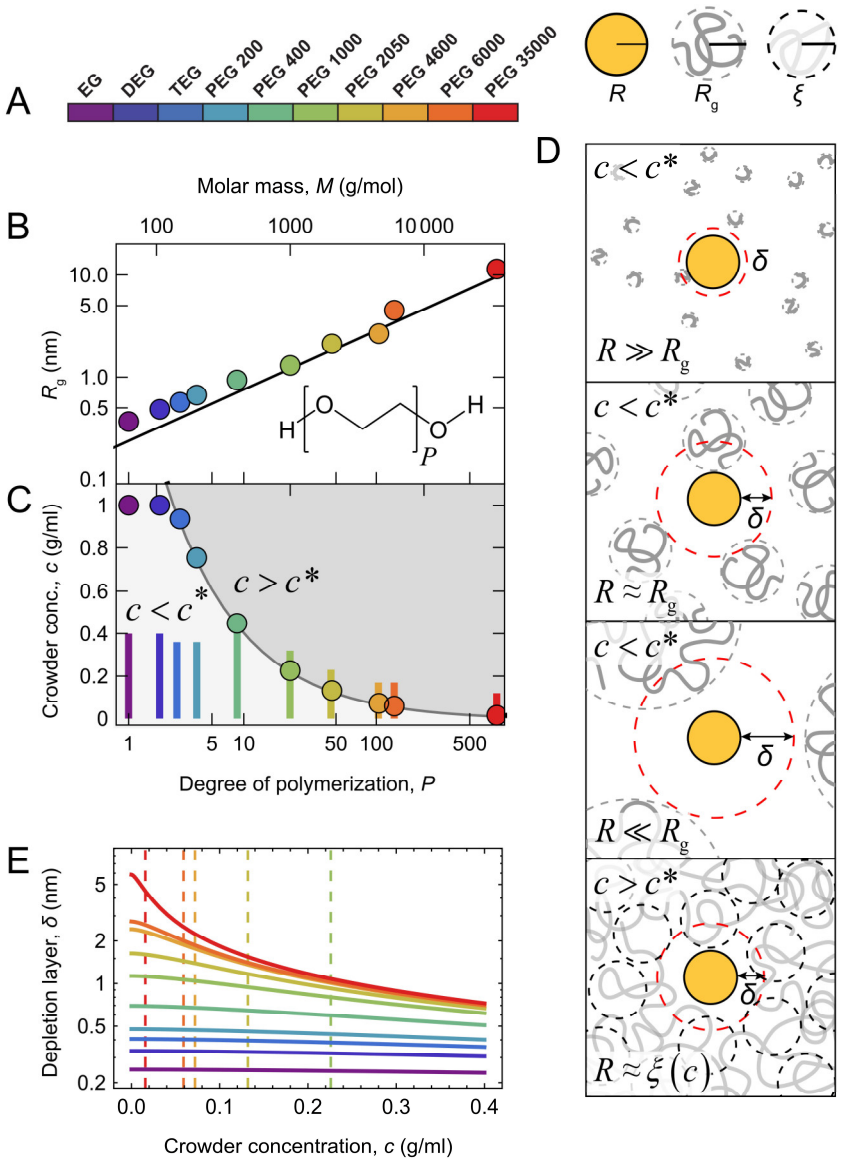

Figure S1. Polymeric crowders and the depletion layer. (*A*) Color legend for PEGs with different molar masses. (*B*) Radius of gyration, R_g, plotted against the degree of polymerization, P, and the molar mass, M, of PEG[1,2], and a fit with the scaling law $R_g = 0.21\ \text{nm} \cdot P^{0.583}$.[3] Deviations from the fit (which was obtained for PEG molecules over the entire range of lengths originally reported[3]) are due to finite-length effects for small values of P. The structural formula of PEG is given in the inset. (*C*) *Line*: overlap concentration, c^*, calculated from Eq. (1) with $R_g = 0.21\ \text{nm} \cdot P^{0.583}$, Circles: c^* calculated based on published R_g values[1-3]. *Bars*: Ranges of PEG concentrations probed here. (*D*) The depletion layer around a colloidal particle (modeled as hard spheres of radius *R*, orange) in solution with polymers of radius of gyration R_g (gray). The thickness of the depletion layer, δ, is visualized for several regimes: For $R \gg R_g$ (top panel), the depletion layer is given by Eq. (9) and increases with crowder size (second and third panels); for $R \approx R_g$, Eq. (10) is valid. In the semidilute regime ($c > c^*$, fourth panel), the polymer chains overlap and form a network with a mesh size given by the correlation length $\xi = R_g (c / c^*)^{-0.77}$, resulting in $\delta = \xi$. (*E*) δ (calculated around a sphere with *R*=2 nm) as a function of the PEG concentration for every size of PEG used, with the respective overlap concentrations indicated as dashed lines.

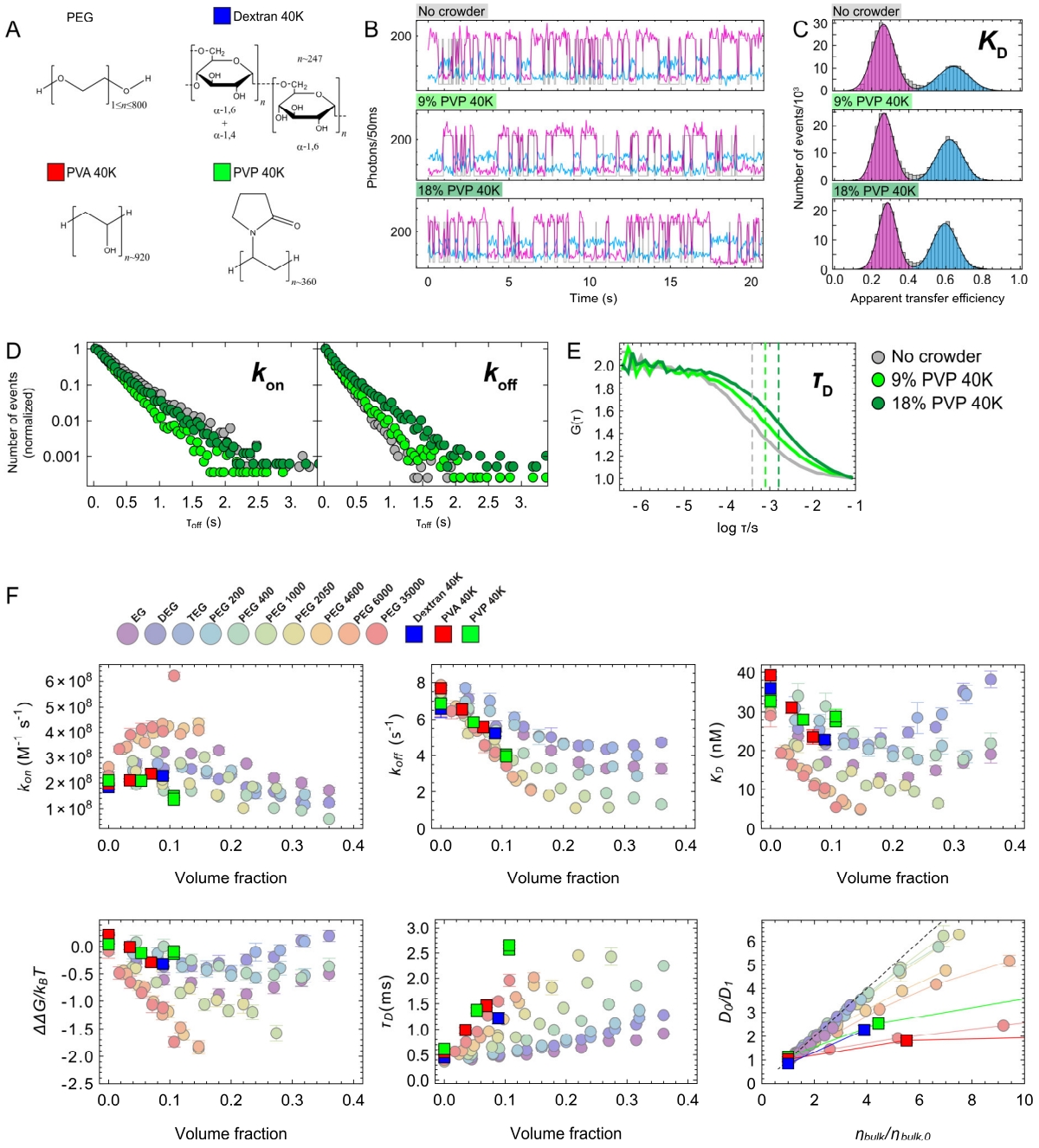

Figure S2. Comparison of PEG to other polymeric crowders. (A) Chemical structures of PEG (EG-PEG 35000), dextran with an average molar mass of 40 kg/mol (Dextran 40K, blue square), polyvinyl alcohol with an average molar mass of 40.5 kg/mol (PVA 40K, red square), and polyvinylpyrrolidone with an average molar mass of 40 kg/mol (PVP 40K, green). Note that PEG, PVA, and PVP are linear polymers, whereas dextran is branched. (*B-E*) Examples of single-molecule measurements with immobilized donor-labeled ACTR molecules binding to acceptor-labeled NCBD (c.f. Fig. 1*A*) at three different concentrations of PVP 40K: 0% (gray), 9% (light green), and 18% (dark green). (*B*) Examples of time traces of association and dissociation, with the donor signal in magenta and the acceptor signal in light blue (first 20s each, binning: 50ms; not corrected for background, quantum yields, detection efficiencies, etc.). The gray lines represent the most likely state trajectories (bound and unbound) as determined by the Viterbi algorithm. (*C*) The time traces were binned at 20ms and combined to an apparent transfer efficiency histogram, from which the equilibrium dissociation constant, K_D can be obtained. (*D*) Normalized dwell-time distributions based on the Viterbi-assigned states of 52-79 molecules per condition for the unbound (left panel) and the bound states (right panel) to yield k_{on} and

k_{off}, respectively. (*E*) Normalized FCS curves of the three conditions used in (*B*). The diffusion times (dashed lines) report on the translational diffusion of NCBD at the different conditions. (F) Binding experiments of ACTR and NCBD in the presence of different concentrations of Dextran 40K (blue), PVA 40K (red), and PVP 40K (green). For comparison, the experiments with the different PEGs as crowders are shown as circles (see legend for PEG sizes). Since the different crowders have very different monomer sizes, we show the dependencies of our observables as a function of volume fraction. The analysis with 1-ms binning in combination with the maximum-likelihood approach based on a hidden Markov model was used for obtaining the association rate coefficient (k_{on}), dissociation rate coefficient (k_{off}), equilibrium dissociation constant (K_D), and the change in interaction free energy ($\Delta\Delta G/k_BT$). The diffusion times (τ_D) represent the mean of two measurements and the error bars indicate the span. In the last panel, the relation between relative bulk viscosity ($\eta_{bulk}/\eta_{bulk,0}$) and the relative microviscosity is shown (c.f. Fig. 3).

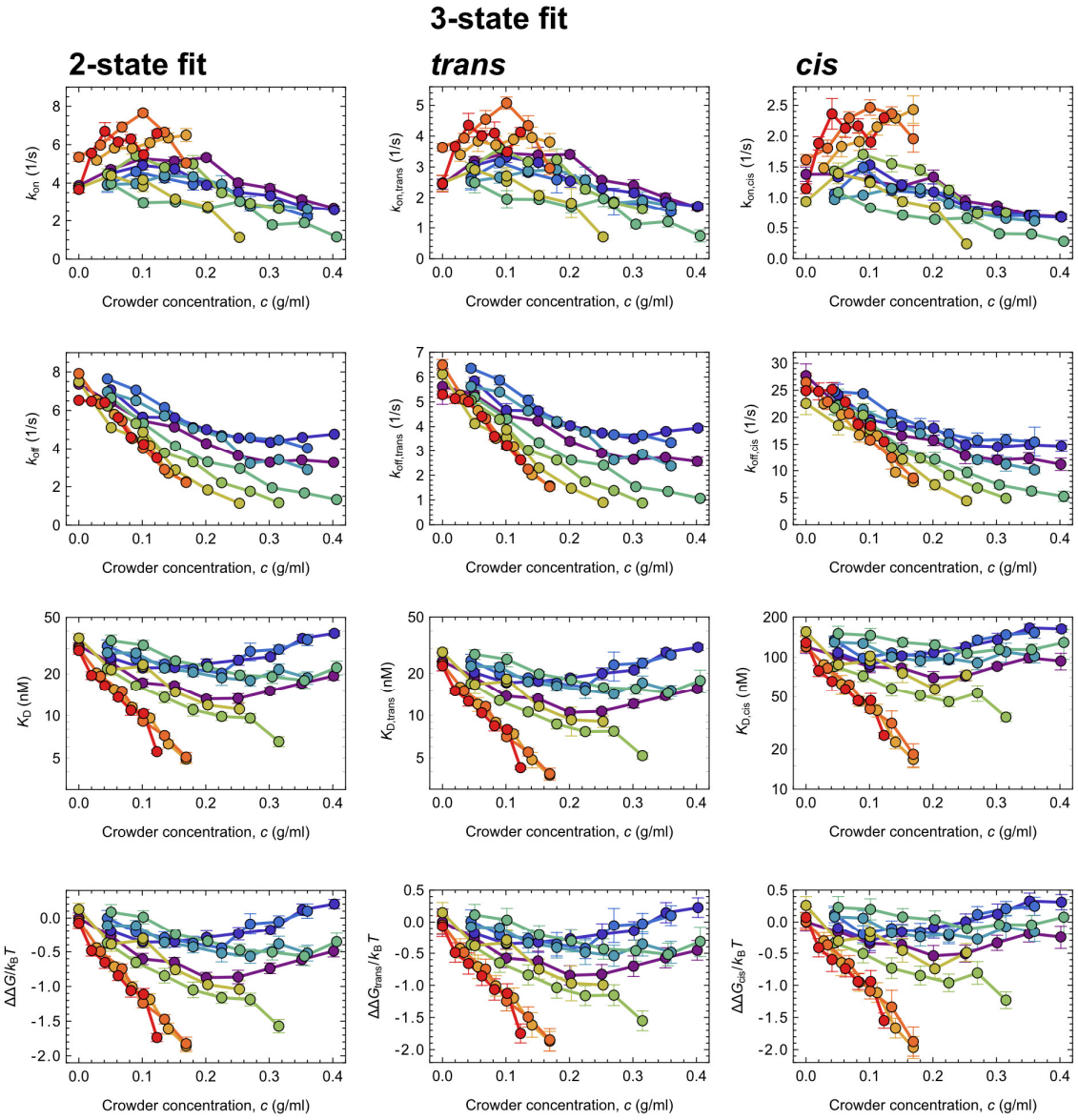

Figure S3. Comparison of kinetic and equilibrium parameters obtained from maximum likelihood analysis using either a two-state model (Eq. 17, left column) or a three-state model (Eq. 16, middle and right columns). The three-state analysis assumes that NCBD can exist in two conformations that differ in the configuration of a proline residue (trans or cis)[4]. In the two-state analysis (which we focus on in the main text for the sake of clarity), the two conformations are treated as equivalent in terms of their response to crowding, which is supported by this comparison. See Methods for details.

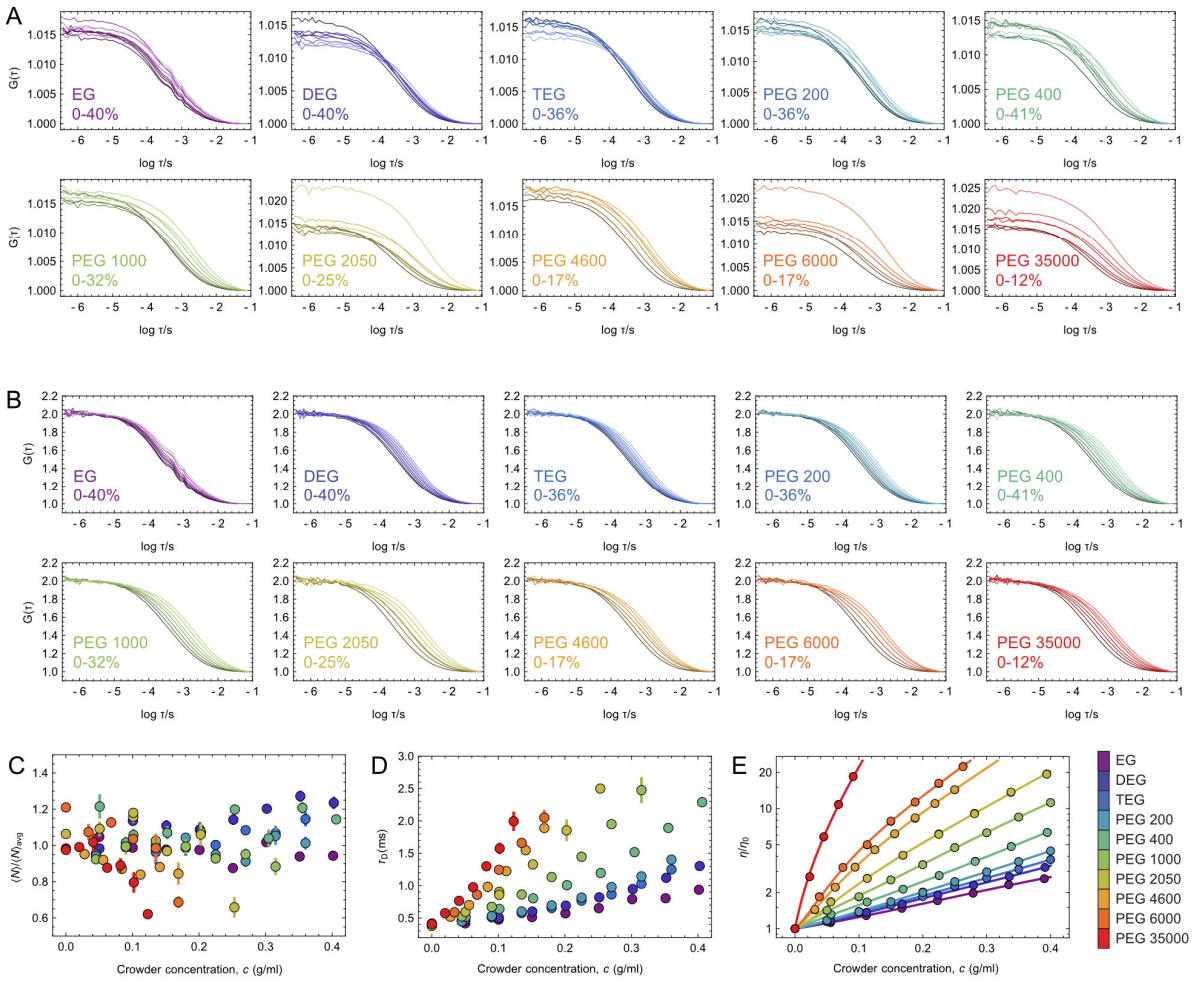

Figure S4. FCS measurements of freely diffusing NCBD. (*A*) Raw data. Two measurements were done per PEG concentration (one before and one after recording surface trajectories); their respective average is displayed. Lighter colors indicate increasing PEG concentrations, with the corresponding range indicated in each plot. All FCS curves were fitted with a free amplitude, a diffusion term, and a triplet term (shared among all fits, see Materials and Methods). The resulting values were used to quantify the change in viscosity as well as the concentration of NCBD. (*B*) FCS curves normalized to an amplitude of 1 to illustrate the increase in diffusion time with increasing PEG concentration. (*C*) Mean number of molecules in the confocal volume, $\langle N \rangle$, normalized by the average over all measurements, $\langle N \rangle_{\mathrm{avg}}$ (*Materials and Methods*), plotted against the PEG concentration. Data points are the mean of two measurements, error bars indicate the span. For large PEGs (2050, 6000, 35000), there is a significant decrease in the number of NCBD molecules at high PEG concentrations. This effect is probably caused by adsorption of NCBD to the coverslip surface, as single molecule trajectories recorded under these conditions also display a significantly higher background in the acceptor channel. (*D*) Diffusion time of NCBD, plotted against the PEG concentration. Data points are the mean of two measurements, error bars indicate the span. (*E*) Bulk viscosities as a function of the PEG concentration, as measured by a shear-flow viscometer. The lines are polynomial interpolations of the data that were used as reference for fitting microviscosities.

Table S1. Experimental parameters recorded for the PEG titration series, as well as for the other crowders. *1st column*: Concentration of crowder. *2nd column*: total recording time of the experiment. *3rd column*: concentration of NCBD determined as the mean of two FCS measurements (error reflects the span of the measurements). *4th column*: viscosity relative to the viscosity in phosphate buffer (η/η_0), determined from the mean diffusion time of NCBD in two FCS experiments (error reflects the span of the measurements). *5-6th column*: fraction bound, determined from transfer efficiency histograms (histo) or rate coefficients (rates). *7th-9th column*: association and dissociation rate coefficients, and equilibrium dissociation constant, determined from a fit with a two-state model. *10th-15th column*: association and dissociation rate coefficients, and equilibrium dissociation constants, determined from a fit with a three-state model. Errors are propagated from the associated parameters.

50 mM sodium phosphate buffer														
C (g/ml)	total time (s)	c_{NCBD} (nM)	η/η_0	frac. bound (histo)	frac. bound (rates)	k_{on} (s^{-1})	k_{off} (s^{-1})	K_D (nM)	$k_{on,1}$ (s^{-1})	$k_{on,2}$ (s^{-1})	$k_{off,1}$ (s^{-1})	$k_{off,2}$ (s^{-1})	$K_{D,1}$ (nM)	$K_{D,2}$ (nM)
0	2033	16.3±0.2	0.97±0.03	0.33	0.34±0.02	3.8±0.1	7.4±0.6	31.4±2.6	2.4±0.2	1.4±0.1	5.6±0.7	27.7±2.2	24.1±3.5	118±13
0	2468	17.7±0.2	0.95±0.03	0.33	0.33±0.02	3.7±0.2	7.5±0.3	35.2±2.7	2.5±0.3	0.9±0.1	6.1±0.2	22.6±2.1	27.9±1.8	153±13
0	2600	20.1±0.1	1.05±0.05	0.40	0.40±0.02	5.3±0.2	7.9±0.2	29.8±1.2	3.6±0.1	1.6±0.1	6.5±0.2	26.5±1.7	23.0±0.7	118±11
0	3263	16.2±0.2	1.03±0.03	0.35	0.36±0.03	3.7±0.3	6.6±0.5	29.0±2.9	2.5±0.3	1.1±0.1	5.3±0.1	24.9±2.8	22.3±1.7	126±16
Ethylene glycol														
C (g/ml)	total time (s)	c_{NCBD} (nM)	η/η_0	frac. bound (histo)	frac. bound (rates)	k_{on} (s^{-1})	k_{off} (s^{-1})	K_D (nM)	$k_{on,1}$ (s^{-1})	$k_{on,2}$ (s^{-1})	$k_{off,1}$ (s^{-1})	$k_{off,2}$ (s^{-1})	$K_{D,1}$ (nM)	$K_{D,2}$ (nM)
0.05	2356	17.4±0.1	1.05±0.00	0.42	0.42±0.02	4.8±0.2	6.5±0.2	23.7±1.3	3.2±0.2	1.4±0.1	5.3±0.2	22.2±1.6	18.5±0.7	101±10
0.1	2563	16.4±0.2	1.20±0.03	0.49	0.49±0.02	5.3±0.2	5.5±0.1	17.0±0.7	3.4±0.1	1.3±0.1	4.4±0.1	18.1±1.2	13.5±0.4	83±8
0.151	2467	16.2±0.2	1.30±0.04	0.50	0.50±0.02	5.1±0.2	5.1±0.1	16.2±0.6	3.4±0.3	1.2±0.1	4.2±0.1	16.6±1.4	13.0±0.6	82±5
0.201	3245	16.2±0.1	1.44±0.03	0.55	0.55±0.03	5.3±0.2	4.3±0.2	13.0±0.8	3.4±0.1	1.3±0.1	3.4±0.1	15.8±1.0	10.3±0.4	69±8
0.251	2530	14.5±0.3	1.64±0.01	0.53	0.53±0.02	4.0±0.1	3.6±0.2	13.1±0.6	2.6±0.1	0.9±0.1	2.9±0.1	12.8±1.5	10.5±0.5	71±6
0.301	3253	16.9±0.1	1.99±0.00	0.53	0.53±0.04	3.7±0.2	3.3±0.2	14.9±1.2	2.4±0.2	0.9±0.0	2.6±0.0	12.0±0.6	11.9±0.8	84±4
0.351	3293	15.6±0.1	2.03±0.00	0.48	0.48±0.04	3.1±0.2	3.4±0.1	16.9±1.4	2.0±0.1	0.7±0.0	2.7±0.1	12.3±1.0	13.6±0.8	97±8
0.401	4283	15.7±0.3	2.36±0.00	0.45	0.45±0.04	2.7±0.2	3.3±0.3	19.0±2.3	1.7±0.1	0.7±0.0	2.6±0.2	11.2±1.1	15.3±0.7	92±13
Diethylene glycol														
C (g/ml)	total time (s)	c_{NCBD} (nM)	η/η_0	frac. bound (histo)	frac. bound (rates)	k_{on} (s^{-1})	k_{off} (s^{-1})	K_D (nM)	$k_{on,1}$ (s^{-1})	$k_{on,2}$ (s^{-1})	$k_{off,1}$ (s^{-1})	$k_{off,2}$ (s^{-1})	$K_{D,1}$ (nM)	$K_{D,2}$ (nM)
0.05	2681	16.3±0.2	1.16±0.06	0.38	0.39±0.03	4.5±0.3	7.1±0.3	25.6±1.8	3.1±0.2	1.3±0.1	5.8±0.1	24.2±1.9	20.0±0.9	106±11
0.101	2568	18.8±0.3	1.28±0.02	0.46	0.46±0.03	4.9±0.2	5.6±0.3	21.7±1.6	3.3±0.2	1.5±0.1	4.7±0.3	19.6±0.8	16.9±0.6	87±9
0.151	3989	18.4±0.4	1.51±0.02	0.45	0.46±0.02	4.7±0.2	5.6±0.1	21.9±1.1	3.1±0.3	1.2±0.1	4.6±0.1	18.4±0.7	17.3±1.1	101±5
0.201	3841	18.1±0.5	1.74±0.00	0.43	0.44±0.03	3.9±0.2	5.0±0.5	23.2±2.6	2.5±0.2	1.1±0.1	4.0±0.1	18.0±1.3	18.3±1.0	107±14
0.252	4248	19.0±0.3	2.07±0.01	0.43	0.43±0.02	3.5±0.2	4.5±0.2	24.6±1.5	2.3±0.2	0.9±0.0	3.7±0.1	14.9±0.9	19.7±1.9	118±7
0.302	2883	20.0±0.1	2.39±0.01	0.43	0.43±0.01	3.3±0.1	4.3±0.1	26.0±0.7	2.2±0.1	0.8±0.0	3.5±0.1	14.5±1.6	20.8±0.9	133±16
0.352	3868	21.1±0.4	2.82±0.02	0.37	0.38±0.02	2.7±0.2	4.6±0.1	35.1±2.1	1.8±0.2	0.7±0.0	3.8±0.1	14.9±1.0	27.9±1.8	163±11
0.402	3033	20.5±0.4	3.28±0.03	0.35	0.35±0.02	2.5±0.1	4.7±0.1	38.1±2.1	1.7±0.1	0.7±0.0	3.9±0.1	14.7±1.1	30.2±1.5	161±9
Triethylene glycol														
C (g/ml)	total time (s)	c_{NCBD} (nM)	η/η_0	frac. bound (histo)	frac. bound (rates)	k_{on} (s^{-1})	k_{off} (s^{-1})	K_D (nM)	$k_{on,1}$ (s^{-1})	$k_{on,2}$ (s^{-1})	$k_{off,1}$ (s^{-1})	$k_{off,2}$ (s^{-1})	$K_{D,1}$ (nM)	$K_{D,2}$ (nM)
0.045	4140	15.8±0.3	1.16±0.02	0.33	0.34±0.03	3.9±0.4	7.7±0.2	31.0±2.9	2.6±0.4	1.1±0.1	6.4±0.1	24.8±1.7	24.3±2.6	132±9
0.09	3308	16.4±0.3	1.29±0.02	0.39	0.39±0.03	4.5±0.3	7.0±0.4	25.3±2.1	3.2±0.2	1.5±0.1	5.9±0.2	24.4±0.4	19.6±1.2	97±8
0.135	4640	16.0±1.0	1.46±0.02	0.40	0.41±0.02	4.2±0.1	6.1±0.3	23.2±1.2	2.8±0.1	1.1±0.1	5.1±0.2	20.6±0.8	18.4±0.5	106±6
0.18	4414	16.4±0.6	1.65±0.02	0.43	0.43±0.04	3.9±0.4	5.1±0.1	21.4±2.0	2.6±0.4	1.1±0.1	4.1±0.1	18.4±1.4	16.8±1.9	100±9
0.225	4547	16.6±0.2	1.94±0.03	0.45	0.45±0.02	3.9±0.2	4.7±0.1	20.0±1.1	2.6±0.2	1.1±0.0	3.8±0.1	16.9±1.0	15.7±1.0	94±6
0.27	4212	18.0±0.1	2.18±0.00	0.38	0.39±0.06	2.9±0.4	4.6±0.2	28.4±4.0	1.9±0.4	0.8±0.1	3.7±0.1	15.8±1.3	22.7±5.2	133±8

0.315	3723	17.7±0.5	2.59±0.02	0.37	0.38±0.02	2.7±0.1	4.4±0.1	29.4±1.6	1.8±0.2	0.7±0.0	3.7±0.1	15.9±1.0	23.4±1.9	145±5
0.36	3771	19.0±0.5	3.15±0.09	0.35	0.36±0.02	2.2±0.1	4.0±0.1	34.4±2.3	1.5±0.1	0.7±0.1	3.4±0.1	15.5±2.7	26.6±1.5	151±14

PEG 200

C (g/ml)	total time (s)	c_{NCBD} (nM)	η/η_0	frac. bound (histo)	frac. bound (rates)	k_{on} (s^{-1})	k_{off} (s^{-1})	K_D (nM)	$k_{on,1}$ (s^{-1})	$k_{on,2}$ (s^{-1})	$k_{off,1}$ (s^{-1})	$k_{off,2}$ (s^{-1})	$K_{D,1}$ (nM)	$K_{D,2}$ (nM)
0.045	4409	15.6±0.3	1.13±0.03	0.35	0.36±0.02	3.9±0.2	7.0±0.2	27.8±1.8	2.5±0.2	1.0±0.0	5.6±0.2	22.1±1.6	22.2±1.8	128±10
0.09	4776	16.8±0.4	1.34±0.01	0.37	0.38±0.02	3.9±0.2	6.5±0.1	27.7±1.7	2.7±0.2	1.0±0.0	5.4±0.1	21.5±1.0	21.9±1.5	125±5
0.135	2727	16.6±0.3	1.52±0.02	0.43	0.43±0.03	4.3±0.2	5.7±0.2	21.7±1.5	2.9±0.1	1.2±0.1	4.6±0.2	19.0±1.3	17.2±0.9	99±5
0.18	3397	17.3±0.2	1.75±0.03	0.46	0.46±0.03	4.3±0.1	5.0±0.4	20.3±1.8	2.9±0.3	1.1±0.1	4.2±0.2	17.0±0.9	16.0±1.3	93±9
0.225	3622	15.8±0.3	2.06±0.00	0.46	0.46±0.04	3.9±0.3	4.6±0.1	18.5±1.4	2.6±0.4	0.9±0.1	3.8±0.1	15.3±1.3	14.8±1.9	96±6
0.27	4964	15.2±0.4	2.47±0.01	0.46	0.46±0.02	2.7±0.1	3.2±0.1	17.7±1.1	1.8±0.1	0.7±0.1	2.6±0.1	12.0±0.7	14.0±1.1	89±10
0.315	4477	17.5±0.7	2.88±0.03	0.45	0.45±0.04	2.8±0.2	3.4±0.2	21.2±2.0	1.9±0.3	0.7±0.0	2.9±0.1	11.2±1.3	16.9±2.0	108±18
0.36	4293	16.8±0.5	3.53±0.01	0.48	0.48±0.04	2.6±0.2	2.9±0.2	18.5±1.6	1.7±0.2	0.6±0.0	2.4±0.1	10.1±0.6	14.8±1.4	100±11

PEG 400

C (g/ml)	total time (s)	c_{NCBD} (nM)	η/η_0	frac. bound (histo)	frac. bound (rates)	k_{on} (s^{-1})	k_{off} (s^{-1})	K_D (nM)	$k_{on,1}$ (s^{-1})	$k_{on,2}$ (s^{-1})	$k_{off,1}$ (s^{-1})	$k_{off,2}$ (s^{-1})	$K_{D,1}$ (nM)	$K_{D,2}$ (nM)
0.051	3059	20.2±1.0	1.31±0.02	0.37	0.37±0.03	3.9±0.3	6.6±0.2	34.0±3.2	2.5±0.3	1.1±0.1	5.2±0.2	22.2±3.0	26.9±2.1	148±20
0.101	3049	17.5±0.4	1.61±0.00	0.35	0.36±0.04	3.0±0.3	5.4±0.3	31.5±3.3	2.0±0.3	0.8±0.0	4.3±0.1	18.9±2.2	24.8±2.8	144±18
0.152	3404	17.8±0.5	2.03±0.01	0.42	0.42±0.03	3.0±0.2	4.1±0.2	24.4±1.9	1.9±0.1	0.7±0.0	3.3±0.1	14.1±0.6	19.5±0.8	127±10
0.203	3063	17.8±0.3	2.54±0.07	0.44	0.45±0.03	2.7±0.1	3.3±0.2	22.0±1.6	1.7±0.2	0.6±0.0	2.6±0.1	12.1±1.3	17.7±1.7	122±11
0.254	3090	19.9±0.3	3.01±0.04	0.50	0.51±0.04	3.0±0.2	2.9±0.1	19.3±1.7	2.0±0.3	0.7±0.1	2.4±0.1	9.7±1.0	15.6±1.1	105±6
0.305	4161	17.2±0.7	3.82±0.09	0.48	0.48±0.04	1.8±0.1	1.9±0.1	18.8±1.5	1.1±0.1	0.4±0.0	1.5±0.0	7.4±0.6	15.2±1.3	113±4
0.355	4391	20.1±0.4	4.77±0.09	0.53	0.53±0.07	1.9±0.2	1.7±0.1	17.7±2.1	1.2±0.2	0.4±0.0	1.3±0.0	6.2±0.7	14.3±1.4	112±11
0.406	2798	19.0±0.2	5.77±0.01	0.46	0.47±0.06	1.2±0.1	1.3±0.1	21.8±2.8	0.7±0.2	0.3±0.0	1.1±0.1	5.2±1.0	17.5±3.3	127±32

PEG 1000

C (g/ml)	total time (s)	c_{NCBD} (nM)	η/η_0	frac. bound (histo)	frac. bound (rates)	k_{on} (s^{-1})	k_{off} (s^{-1})	K_D (nM)	$k_{on,1}$ (s^{-1})	$k_{on,2}$ (s^{-1})	$k_{off,1}$ (s^{-1})	$k_{off,2}$ (s^{-1})	$K_{D,1}$ (nM)	$K_{D,2}$ (nM)
0.045	3836	15.3±0.2	1.32±0.02	0.41	0.42±0.03	4.4±0.2	6.2±0.2	21.5±1.4	3.0±0.2	1.4±0.1	5.1±0.1	21.8±1.1	16.7±1.1	84±3
0.09	3451	16.5±0.6	1.69±0.00	0.50	0.50±0.02	5.4±0.2	5.3±0.1	16.3±0.5	3.6±0.1	1.7±0.2	4.3±0.1	20.4±2.1	12.6±0.4	71±7
0.135	3853	17.0±0.5	2.18±0.00	0.56	0.56±0.02	4.7±0.1	3.7±0.2	13.4±0.8	3.2±0.1	1.6±0.1	3.0±0.2	14.3±0.8	10.4±0.6	57±7
0.18	3515	16.5±0.5	2.85±0.06	0.60	0.60±0.05	5.0±0.3	3.3±0.1	10.9±0.7	3.2±0.3	1.5±0.1	2.6±0.1	12.4±0.9	8.5±0.6	51±5
0.225	4691	15.4±0.3	3.64±0.01	0.61	0.61±0.03	3.4±0.2	2.2±0.1	9.8±0.6	2.3±0.1	1.1±0.1	1.7±0.1	9.1±0.6	7.5±0.4	45±4
0.27	4981	15.8±0.4	4.91±0.09	0.63	0.63±0.05	2.9±0.2	1.8±0.1	9.5±0.9	1.8±0.2	0.7±0.1	1.4±0.1	6.8±0.4	7.6±0.6	53±7
0.315	4181	14.7±0.7	6.23±0.45	0.68	0.69±0.08	2.6±0.3	1.2±0.1	6.5±0.7	1.6±0.1	0.8±0.1	0.9±0.0	4.9±0.2	5.1±0.3	34±3

PEG 2050

C (g/ml)	total time (s)	c_{NCBD} (nM)	η/η_0	frac. bound (histo)	frac. bound (rates)	k_{on} (s^{-1})	k_{off} (s^{-1})	K_D (nM)	$k_{on,1}$ (s^{-1})	$k_{on,2}$ (s^{-1})	$k_{off,1}$ (s^{-1})	$k_{off,2}$ (s^{-1})	$K_{D,1}$ (nM)	$K_{D,2}$ (nM)
0.051	3606	18.1±0.5	1.50±0.08	0.46	0.46±0.03	4.5±0.3	5.2±0.3	21.1±1.7	2.9±0.4	1.4±0.2	4.1±0.2	18.5±1.7	16.4±2.3	87±9
0.101	4186	19.2±0.4	2.28±0.12	0.45	0.46±0.03	3.8±0.2	4.4±0.2	22.4±1.6	2.5±0.4	1.3±0.1	3.6±0.2	16.8±1.6	17.3±2.2	92±10
0.101	2287	19.6±0.1	2.16±0.10	0.46	0.46±0.04	4.2±0.2	4.9±0.5	22.9±2.7	2.7±0.2	1.2±0.2	3.9±0.1	17.7±1.0	18.0±0.9	100±8
0.152	3089	16.1±0.2	3.34±0.11	0.52	0.52±0.04	3.2±0.2	2.9±0.1	14.7±1.0	2.1±0.2	0.9±0.1	2.3±0.1	12.1±1.2	11.4±0.7	75±11
0.203	3420	17.6±0.9	4.67±0.37	0.60	0.60±0.05	2.7±0.2	1.8±0.1	11.8±1.0	1.8±0.5	0.8±0.1	1.5±0.0	7.4±0.9	9.1±2.1	56±6
0.253	3490	10.9±0.8	6.30±0.00	0.50	0.50±0.07	1.1±0.1	1.1±0.1	11.0±1.5	0.7±0.1	0.2±0.0	0.9±0.0	4.4±0.6	8.9±0.8	72±6

PEG 4600

C (g/ml)	total time (s)	c_{NCBD} (nM)	η/η_0	frac. bound (histo)	frac. bound (rates)	k_{on} (s^{-1})	k_{off} (s^{-1})	K_D (nM)	$k_{on,1}$ (s^{-1})	$k_{on,2}$ (s^{-1})	$k_{off,1}$ (s^{-1})	$k_{off,2}$ (s^{-1})	$K_{D,1}$ (nM)	$K_{D,2}$ (nM)
0.028	4803	15.8±0.4	1.31±0.01	0.43	0.44±0.02	5.3±0.2	6.7±0.3	20.0±1.3	3.4±0.2	1.5±0.1	5.3±0.1	22.5±0.7	15.7±0.7	86±7
0.056	3249	15.3±0.3	1.76±0.04	0.49	0.50±0.01	5.8±0.1	5.8±0.2	15.3±0.6	3.8±0.3	1.8±0.2	4.6±0.3	20.5±1.3	11.8±1.3	62±10

0.084	2801	14.5±0.3	2.47±0.15	0.56	0.56±0.03	5.7±0.2	4.5±0.3	11.4±0.8	3.7±0.3	1.9±0.1	3.5±0.1	16.7±1.3	8.8±0.6	46±4
0.112	3052	13.9±0.1	3.08±0.03	0.59	0.59±0.03	5.9±0.2	4.1±0.2	9.6±0.6	3.9±0.2	2.1±0.1	3.2±0.1	16.6±0.9	7.3±0.4	39±4
0.141	3669	14.6±0.3	3.90±0.14	0.70	0.70±0.03	6.1±0.2	2.6±0.1	6.3±0.3	4.0±0.3	2.3±0.1	2.0±0.1	9.7±0.7	4.8±0.6	22±2
0.169	4279	14.0±0.9	4.76±0.10	0.71	0.74±0.04	6.1±0.3	2.2±0.1	4.9±0.3	3.8±0.3	2.4±0.2	1.6±0.1	7.9±0.6	3.7±0.2	16±2

PEG 6000

C (g/ml)	total time (s)	c_{NCBD} (nM)	η/η_0	frac. bound (histo)	frac. bound (rates)	k_{on} (s^{-1})	k_{off} (s^{-1})	K_D (nM)	$k_{on,1}$ (s^{-1})	$k_{on,2}$ (s^{-1})	$k_{off,1}$ (s^{-1})	$k_{off,2}$ (s^{-1})	$K_{D,1}$ (nM)	$K_{D,2}$ (nM)
0.034	3917	17.8±0.6	1.49±0.00	0.48	0.48±0.03	6.1±0.3	6.5±0.3	19.1±1.2	3.9±0.1	1.8±0.1	5.1±0.2	22.9±1.4	14.8±0.6	81±7
0.068	2665	18.7±0.3	2.16±0.02	0.55	0.56±0.02	6.7±0.2	5.4±0.2	14.9±0.7	4.5±0.3	2.3±0.1	4.3±0.1	20.7±0.7	11.4±0.7	61±4
0.101	3714	17.2±0.3	3.13±0.02	0.65	0.65±0.02	7.5±0.2	4.0±0.1	9.1±0.3	5.1±0.2	2.5±0.1	3.2±0.1	15.8±0.7	6.9±0.3	40±2
0.135	3504	16.4±1.1	4.18±0.07	0.68	0.69±0.03	6.4±0.2	2.8±0.1	7.2±0.3	4.3±0.3	2.4±0.1	2.2±0.1	12.4±2.1	5.4±0.3	31±7
0.169	2823	11.4±0.4	5.17±0.24	0.68	0.69±0.03	4.7±0.1	2.1±0.1	5.1±0.3	3.0±0.2	2.0±0.2	1.5±0.1	8.6±0.9	3.8±0.4	18±4

PEG 35000

C (g/ml)	total time (s)	c_{NCBD} (nM)	η/η_0	frac. bound (histo)	frac. bound (rates)	k_{on} (s^{-1})	k_{off} (s^{-1})	K_D (nM)	$k_{on,1}$ (s^{-1})	$k_{on,2}$ (s^{-1})	$k_{off,1}$ (s^{-1})	$k_{off,2}$ (s^{-1})	$K_{D,1}$ (nM)	$K_{D,2}$ (nM)
0.02	3461	16.4±0.1	1.45±0.09	0.45	0.46±0.02	5.5±0.2	6.5±0.4	19.3±1.4	3.7±0.1	1.9±0.1	5.1±0.2	24.8±1.6	14.8±0.7	78±7
0.041	4633	16.9±0.7	1.93±0.11	0.50	0.51±0.04	6.6±0.4	6.4±0.3	16.3±1.3	4.4±0.4	2.4±0.2	5.0±0.2	25.1±1.3	12.4±1.0	65±10
0.062	2818	14.6±0.0	2.46±0.08	0.51	0.52±0.04	6.0±0.3	5.6±0.3	13.5±1.0	4.0±0.2	2.1±0.1	4.4±0.2	22.8±1.2	10.3±0.4	56±4
0.082	4258	14.8±0.5	3.27±0.07	0.57	0.58±0.05	6.2±0.4	4.6±0.4	10.9±1.2	4.1±0.4	2.2±0.1	3.6±0.1	18.7±0.5	8.3±0.7	46±3
0.102	3084	13.2±0.8	3.97±0.17	0.56	0.56±0.01	5.4±0.1	4.2±0.2	10.3±0.4	3.5±0.1	1.9±0.1	3.2±0.1	18.4±1.8	7.8±0.3	46±6
0.123	3006	10.3±0.2	5.02±0.32	0.62	0.65±0.02	6.4±0.1	3.4±0.1	5.5±0.2	4.1±0.1	2.3±0.1	2.6±0.0	15.5±1.5	4.2±0.1	25±1

Dextran 40K

C (g/ml)	total time (s)	c_{NCBD} (nM)	η/η_0	frac. bound (histo)	frac. bound (rates)	k_{on} (s^{-1})	k_{off} (s^{-1})	K_D (nM)
0	7315	9.8	0.84	0.21	0.21±0.01	1.8±0.1	6.6±0.5	35.9±2.9
0.09	4533	22.9±1.3	2.26±0.21	0.5	0.50±0.03	5.3±0.2	5.2±0.1	22.8±1.2

PVA 40K

C (g/ml)	total time (s)	c_{NCBD} (nM)	η/η_0	frac. bound (histo)	frac. bound (rates)	k_{on} (s^{-1})	k_{off} (s^{-1})	K_D (nM)
0	5410	11.6±0.2	1.02±0.11	0.22	0.228±0.004	2.27±0.03	7.7±0.1	39.2±0.9
0.045	6174	22.1±0.8	1.83±0.10	0.41	0.42±0.02	4.7±0.1	6.6±0.3	31.1±1.5
0.09	4244	22.5±0.6	2.70±0.06	0.48	0.49±0.04	5.3±0.4	5.6±0.2	23.5±1.9

PVP 40K

C (g/ml)	total time (s)	c_{NCBD} (nM)	η/η_0	frac. bound (histo)	frac. bound (rates)	k_{on} (s^{-1})	k_{off} (s^{-1})	K_D (nM)
0	6697	16.4±0.8	1.14±0.10	0.34	0.33±0.02	3.4±0.1	6.9±0.2	32.7±1.6
0.09	5832	23.4±0.3	2.55±0.09	0.46	0.46±0.01	4.9±0.1	5.9±0.3	28.0±1.4
0.18	5342	25±0.7	4.76±0.18	0.48	0.48±0.01	3.7±0.1	4.1±0.1	27.5±0.8
0.18	3265	22.9±0.4	4.91±0.13	0.45	0.44±0.02	3.2±0.1	4.0±0.2	28.8±1.9

Supporting Information References

1. S Kuga (1981) Pore-Size Distribution Analysis of Gel Substances by Size Exclusion Chromatography. *Journal of Chromatography* 206:449-461.
2. M Hosek & JX Tang (2004) Polymer-induced bundling of F actin and the depletion force. *Phys Rev E Stat Nonlin Soft Matter Phys* 69:051907.
3. K Devanand & JC Selser (1991) Asymptotic-Behavior and Long-Range Interactions in Aqueous-Solutions of Poly(Ethylene Oxide). *Macromolecules* 24:5943-5947.
4. F Sturzenegger, F Zosel, ED Holmstrom, KJ Buholzer, DE Makarov, D Nettels, & B Schuler (2018) Transition path times of coupled folding and binding reveal the formation of an encounter complex. *Nat. Commun.* 9:4708.